

# Growth and Structural Perfection of Epitaxial Nickel Oxide

M. W. VERNON, F. J. SPOONER

*Physics Department, Royal Military College of Science, Shrivenham, Swindon, Wilts, UK*

*Received 10 July 1968, and in revised form 16 August*

Nickel oxide single crystals have been grown epitaxially over a wide range of temperature (270° C) by vapour hydrolysis of nickel bromide on to (001) cleavage faces of magnesium oxide. Results are presented showing the dependence of thickness and surface morphology of the crystal on the reaction temperature and the ratio of water vapour to bromide vapour.

The dislocation density and bulk imperfections in these crystals have been examined using etch-pit and X-ray topographic techniques. The dislocation density over practically the whole range of growth is about  $5 \times 10^7/\text{cm}^2$  and is two orders of magnitude greater than that in the substrate. Above growth temperatures of 640° C, plastic deformation and cleavage of both overgrowth and substrate occurs, and it is shown that thermal stresses induced at the interface on cooling are sufficient for initiation.

Annealing of the crystals on the substrate produces a regular network of slip lines, which influences the antiferromagnetic twin domain structure.

## 1. Introduction

In order to study some physical properties of nickel oxide [1, 2], which is an antiferromagnetic material with a Néel temperature of 523° K [3], single crystals were grown epitaxially by hydrolysis of nickel bromide vapour on to magnesium oxide single crystal substrates. The advantage of these crystals over those grown from the melt is that they are more nearly stoichiometric, although strain may be introduced due to lattice mismatch and differential thermal contraction of the overgrowth and the substrate. Antiferromagnetic domain studies [2] showed that the domain structure was associated with the bulk strain in the NiO, which varied with the thickness of the crystal and subsequent annealing. Although there is considerable theoretical and experimental data on strain and structural imperfections in very thin epitaxial films ( $< 500 \text{ \AA}$ ), there is little information on the bulk strain of thick films ( $> 1 \text{ \mu m}$ ).

Since the bulk strain in thick NiO films, after cooling to room temperature, appeared to depend on the growth temperature, crystals were grown over a wide range of temperature (270° C) with corresponding variations in thickness. The

technique used for growing crystals in the present work resulted in the production of uniformly thick, good surface crystals over practically the whole temperature range used, by suitable adjustment of the ratio of water vapour to bromide vapour. This is in direct conflict with the only other detailed study of epitaxial growth of NiO by Robinson *et al* [4], as their results indicated stringent conditions of substrate and bromide temperature for uniform growth; variations in water vapour pressure having little effect. The results presented here put quantitative limits on the range of good quality growth, and illustrate the effect of the experimental conditions on total thickness, growth rate and quality of these crystals.

Optical, etch-pit and X-ray topographic techniques have been used to study the strain, dislocation density and plastic deformation in both the overgrowth and the substrate. The results presented here show that the appearance of plastic deformation is strongly dependent on the growth temperature, suggesting that differential thermal contraction is the controlling factor rather than lattice mismatch, in common

with the recent work on GaAs/Ge combinations [5].

## 2. Epitaxial Growth

### 2.1. Experimental

The experimental arrangement for crystal growth was similar to that of Cech and Alessandrini [6], deposition taking place inside a vertical fused quartz reaction tube. A preheated cylindrical furnace lowered over the system enabled the working temperature to be reached in a few minutes, and the water vapour pressure was controlled by a steam generator, the system being continuously pumped by a water suction pump. MgO single crystals, from the Norton Co\* and W. and C. Spicer Ltd†, were cleaved into (001) slices and used as substrates, either in the as-cleaved state or after a light etch in conc HCl to remove surface carbonate. The halide and substrate were held at the same temperature in all these experiments, so that varying the reaction temperature changed both the substrate temperature and the vapour pressure of the bromide. Unlike Robinson *et al* [4], single depositions were performed throughout to obviate any possible additional stress induced by the thermal cycling used in multi-deposition techniques.

Early attempts to grow thick crystals with the substrate placed directly over a relatively large quantity of  $\text{NiBr}_2$  (fig. 1a), were hampered because the NiO growth tended to seal off the enclosure between the substrate and the bromide. This prevented further diffusion of water vapour in, and bromide vapour out of the system, and often led to bromide condensing on the crystal surface as it cooled to room temperature. Assum-

ing that the hydrolysis occurs by a heterogeneous reaction on the MgO surface, it is essential for an adequate supply of water vapour to reach the surface for continual growth to occur. Hence, the arrangement shown in fig. 1b was adopted so that (a) a permanent gap could be left around the substrate for ready access of water vapour, and (b) a large quantity of bromide could be used with minimum variation in the substrate-bromide distance. In future this latter arrangement will be referred to as an "open" system and the earlier system as a "closed" one.

### 2.2. Results and Discussion

#### 2.2.1. Open System

The variation of thickness with temperature, using a fixed quantity of nickel bromide and an open system at a water vapour pressure of 25 mm is presented in Graph A of fig. 2. The duration of the experiment was adjusted to ensure complete conversion of bromide to oxide. 7.5 g of bromide were used, and the mass of the deposit corresponding to maximum thickness at temperature  $T_M$  was approximately 0.2 g, representing an efficiency of 15% for conversion of bromide to epitaxially-deposited oxide.

Curve B of fig. 2 shows the effect of increasing the water vapour pressure to 50 mm, where it is seen that  $T_M$  is higher and the thickness at  $T_M$  has increased. In both the above cases, the decrease in thickness with increasing reaction temperature above  $T_M$  is associated with the onset of growth on the sides and back face of the substrate, which increases rapidly with temperature. In fact, the thickness on the back is as great as that on the front face at a reaction

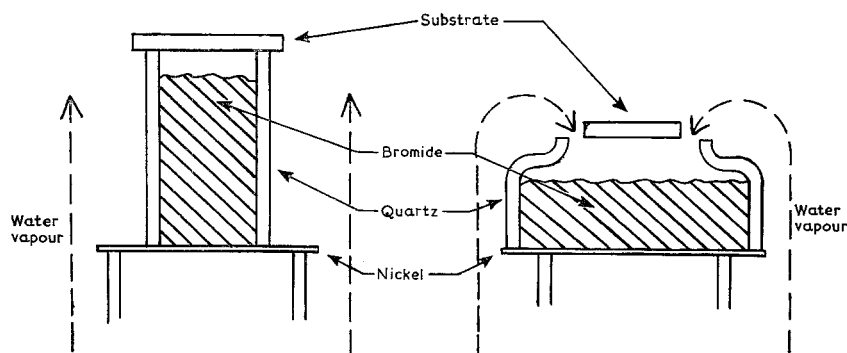


Figure 1 Arrangement of substrate and bromide in (a) the closed system and (b) the open system.

\*Address: Worcester 6, Mass, USA.

†Address: St. Mary's, Winchcomb, Cheltenham, Glos, UK.

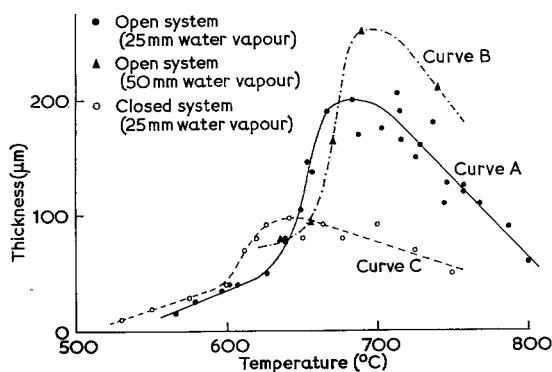


Figure 2 Thickness of growth (front face) as a function of growth temperature under various conditions.

temperature of 750° C. (It must be emphasised that the growth on the front face is uniform in thickness across the whole surface, and it is this thickness only that is used on the graphs.)

The increase in thickness at  $T_M$  on increasing the water vapour pressure suggests that the limiting factor for thick growth on the front face is a deficiency of water vapour in the vicinity of this face. Consequently at higher reaction temperatures, and correspondingly higher bromide vapour pressures, an increasing quantity of bromide vapour escapes from the vicinity of the front face, and either reacts with the water vapour on the sides or back face of the substrate, or escapes completely without reacting.

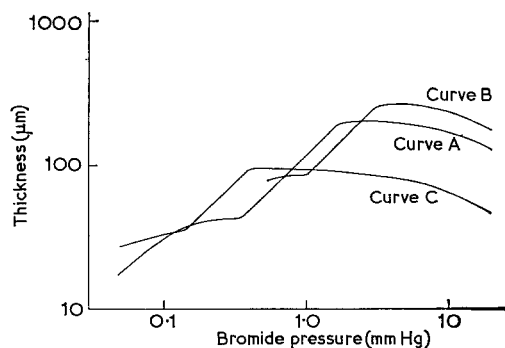


Figure 3 Thickness of growth (front face) as a function of bromide vapour pressure, converted from fig. 2.

The variation of halide vapour pressure with temperature and its effect on the growth is emphasised in fig. 3, where the thicknesses used in curves A and B of fig. 2 are plotted against the vapour pressure of the bromide, the latter being a known function of temperature [7]. It is

apparent that there is a distinct range over which the thickness varies linearly with vapour pressure, this linear region extending up to a vapour pressure corresponding to  $T_M$ . The displacement of the linear regions for the two water vapour pressures suggests that there is a finite range of water pressure and bromide vapour pressure ratio (henceforth denoted  $P_W : P_B$ ) over which the thickness increases most rapidly. The slower increase in thickness at higher and lower values of this ratio is thought to be due to reaction in an excess of water or bromide vapour, and not due to fundamental changes in the growth process. This is supported by fig. 4 which shows that the growth rate varies exponentially with reciprocal temperature over the whole temperature range investigated.

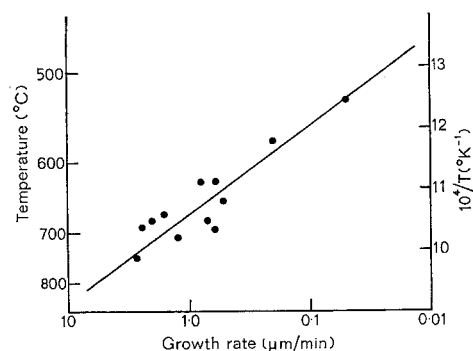


Figure 4 Growth rate as a function of reciprocal growth temperature.

The optical micrographs of fig. 5 are of crystals grown under conditions of curve A of fig. 2, and illustrate that the surface morphology of these crystals is also dependent on the ratio of  $P_W : P_B$ . Over the majority of the range covered by graph A, the surface is basically smooth apart from a regular network of small angle boundaries (fig. 5c). As the excess of water vapour increases, the surface becomes covered with regular square-sided pits (fig. 5b), with the pit edges parallel to  $\langle 110 \rangle$ . Further excess of water vapour leads to a gross breaking up of the surface (fig. 5a), although the epitaxial orientation of the overgrowth is maintained. No regular pitting of the surface is observed in growth under conditions of excess bromide vapour, but the surface becomes rapidly covered with almost circular depressions (fig. 5d), which rapidly grow and merge together, giving the surface a discontinuous appearance.

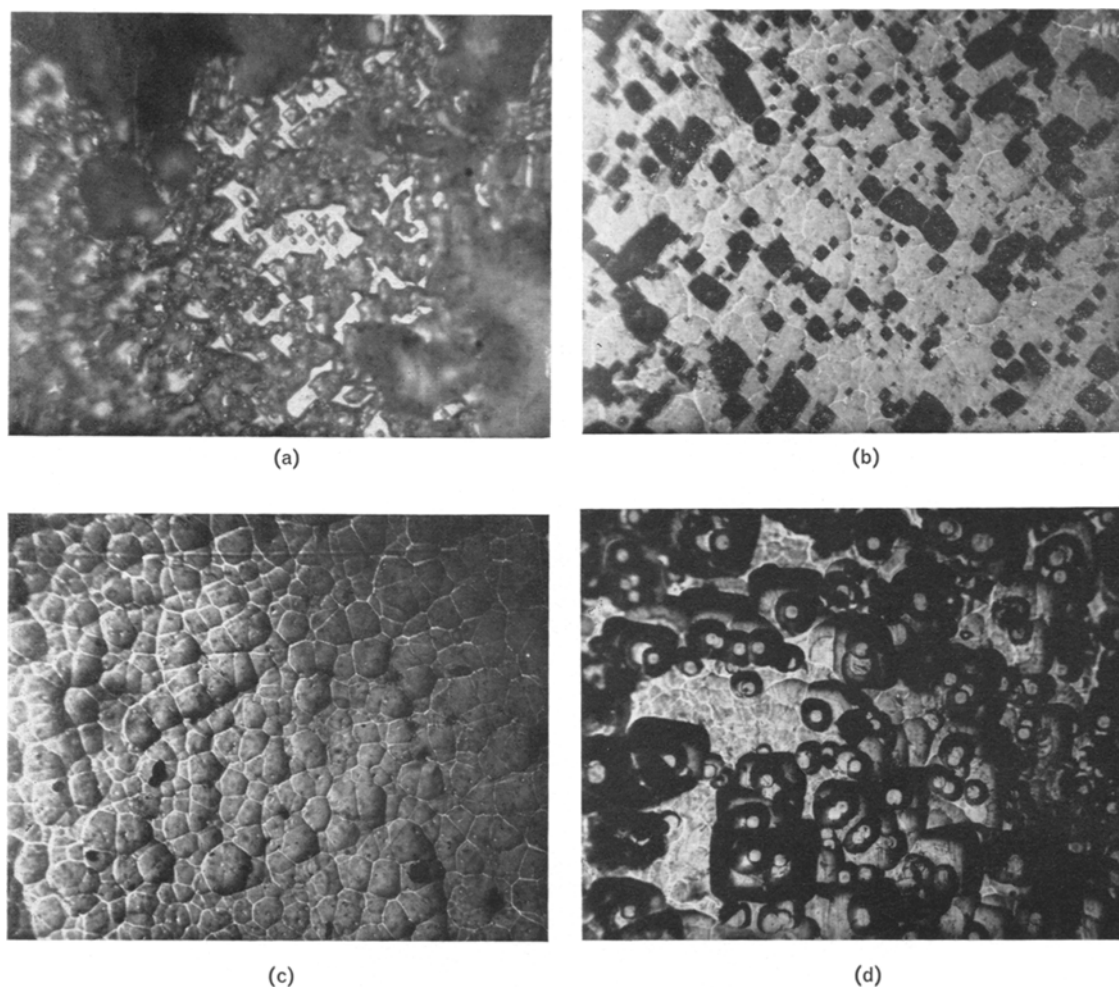


Figure 5 Optical micrographs of growth surfaces of NiO, grown under conditions of graph A of fig. 2. (a) Discontinuous growth at 565° C due to excess water vapour ( $\times 440$ ). (b) Pitted surface at initial stage of excess water vapour, growth temperature 600° C ( $\times 110$ ). (c) Continuous growth at 680° C, showing low-angle boundaries ( $\times 110$ ). (d) Oval depressions due to excess bromide vapour, growth temperature 785° C ( $\times 120$ ).

### 2.2.2. Closed System

The above conclusions on the limits of the growth parameters appear to hold for a closed as well as an open system. For comparison, curves C of figs. 2 and 3 show the variation in thickness with temperature and bromide vapour pressure respectively, for a nominal vapour pressure of 25 mm. To avoid the problems already mentioned regarding a closed system, considerably less initial bromide powder was used (0.6 g giving a deposit mass at  $T_M$  of 0.03 g, representing an efficiency of 25%). The general shape of the curves is unchanged, and again a region of linear variation of thickness with vapour pressure is observed. However, this now occurs over a much lower range of vapour

pressure, suggesting that the actual water vapour pressure in the vicinity of the substrate and bromide is much lower than the 25 mm outside the closed system. The linear regions of graphs A and B occur over a  $P_W : P_B$  ratio of 16 to 50, and if this same ratio is assumed to hold for graph C, then the actual water vapour pressure in the volume enclosed below the substrate is about 6 mm. An advantage of this very low water vapour pressure is that the surface morphology of crystals grown at temperatures as low as 550° C is extremely good, and similar to that shown in fig. 5c, with just a few  $\langle 110 \rangle$  pits randomly distributed across the surface.

Although there is a marked similarity in the variation of thickness with temperature in both

open and closed systems, the thickness of the deposit across the surface is much more uneven in the latter. At low temperatures, the growth is thicker towards the centre, whereas at high temperatures it is vastly enhanced at the edges of the specimen, and the deposit in the central region decreases with increasing growth temperature (the thicknesses used in graphs C are the average thicknesses over this central region). This variation in thickness over the crystal is adequately explained in terms of the  $P_W : P_B$  ratio in the vicinity of the substrate. The bromide vapour cannot escape so easily from a closed system, and there is little or no tendency for growth to occur on the sides or back of the substrate; hence growth occurs preferentially around the edge of the substrate, where  $P_W : P_B$  is a maximum. At low temperatures, maximum thickness occurs in the centre for the same reasons, because under the experimental conditions  $P_W : P_B$  is a minimum in this region.

Robinson *et al* [4] observed similar variations in thickness over a much narrower temperature range, and in fact had zero growth in the centre at a substrate temperature of 680° C, concluding that the enhanced growth at the edge was due to increasing surface diffusion. Moreover, in their experiments the bromide temperature was lower than the substrate temperature, and in view of the present results, the zero growth observed above is probably due to the fact that the  $P_W : P_B$  ratio was much too low at the centre of the substrate.

As a result of their hypothesis of high surface diffusion and the observation of a liquid like intermediate crystallising on the surface, Robinson *et al* [4] proposed that the reaction and subsequent growth occurred via a liquid intermediate. Observations in the present work of the surfaces of over 200 crystals have never revealed signs of liquid droplet solidification, and no experimental evidence for growth occurring via a liquid intermediate. Growth appears to occur by reaction at the substrate surface, and the only limitations on growth are a result of insufficient halide or water vapour in the vicinity of the substrate.

### 3. Structural Perfection

#### 3.1. Experimental

The dislocation density and plastic deformation in both the MgO and the NiO were clearly revealed by etching, the former for 15 sec in 33% hot nitric acid and the latter in 50% hot nitric

for 30 min. The NiO/MgO cross-section could be examined by cleaving normal to the growth surface, imperfections in the substrate being etched and examined first, and those in the overgrowth subsequently. The NiO could be freed completely from the MgO, by dissolving the latter in 20% hot sulphuric acid held just below its boiling point, and subsequent etching enabled both front and back surfaces of the NiO to be examined as well as the cross-section.

X-ray topographs of both (001) surfaces of the NiO were taken with  $\text{CuK}\alpha$  or  $\text{CrK}\alpha$  radiation, using {420}, {311} or {220} reflections and the Berg-Barrett technique [8], using the experimental arrangement described previously [2]. Additional topographs were taken of the dislocation networks above the Néel temperature using a high-temperature cell.

Crystals were examined both optically and topographically in the as-grown state, and after annealing at 1450° C in a low-pressure argon atmosphere in order to simplify the domain structure.

#### 3.2. Observations

##### 3.2.1. Deformation in As-Grown Crystals

The bulk perfection of crystals varied considerably over the range of growth temperatures investigated with regard to the degree of plastic deformation and cleavage observed. At low growth temperatures no macroscopic defects are observed and etching of the cross-section only reveals a random distribution of etch pits in both MgO and NiO (the density in the NiO being about two orders of magnitude higher than in the MgO). Slip lines are first observed at growth temperatures between 630 and 650° C; their density increasing rapidly with increasing growth temperature. The slip lines in the MgO are basically  $\langle 110 \rangle$  and are initiated from, and in close proximity to, the interface (fig. 6). Initially, slip in the NiO consists of short  $\langle 110 \rangle$  traces distributed fairly uniformly throughout the cross-section, but as the growth temperature increases the slip traces lengthen and resemble those in the MgO. The slip lines in the NiO and MgO do not originate from the same point on the interface and those from one do not penetrate the other. A parallel investigation of the surfaces of NiO crystals removed from the substrate revealed only a few randomly distributed  $\langle 100 \rangle$  slip steps in the growth face, and a very complex array of  $\langle 100 \rangle$  slip traces on the back face (fig. 7). The periodicity and regularity

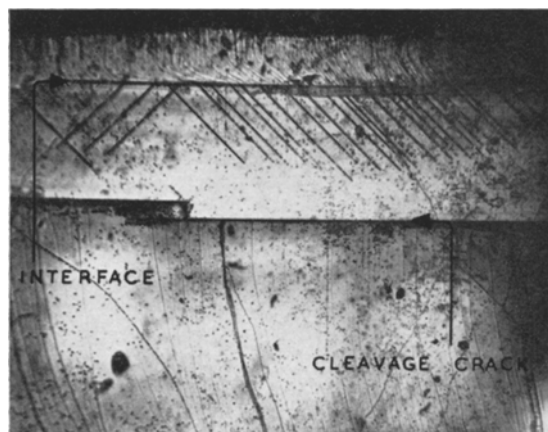


Figure 6 Cross-section of NiO/MgO, showing slip lines in the MgO after etching and cleavage in the substrate parallel to the interface ( $\times 70$ ).

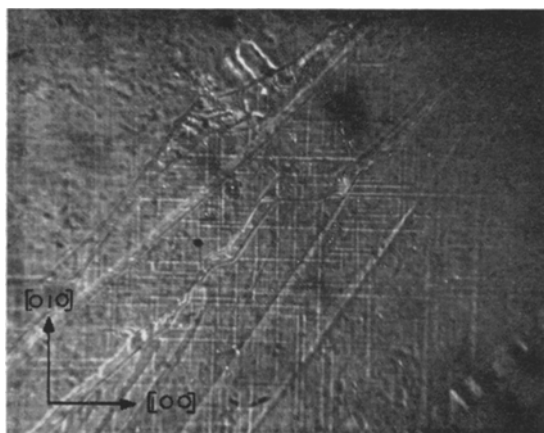


Figure 7 Rectangular network of  $\langle 100 \rangle$  slip traces of  $\{110\}$  slip planes in the back face of an as-grown NiO crystal revealed by phase contrast ( $\times 470$ ).

of this latter structure increases with increasing temperature, but is always too fine to be resolved topographically.

Accompanying the onset of slip, the NiO begins to cleave into rectangular slices; cleavage occurring on  $\{100\}$  planes normal to the interface. Some of the cleavage cracks extend a short distance into the MgO, partially relieving the stress in the MgO near the interface. Additional stress relief occurs in the MgO due to cleavage parallel and close to the interface, as can be seen in fig. 6. The surfaces of the NiO crystals are always slightly concave, as evidenced by the large area, high-resolution topographs that are obtained; this curvature being more pronounced

in the very thin NiO/MgO wafers produced when the parallel cleavage occurs very close to the interface.

The overall dislocation density in the growth surface of the NiO was between  $2$  and  $5 \times 10^7/\text{cm}^2$  over the whole temperature/thickness range, except for crystals less than  $15 \mu\text{m}$  thick, where the density rapidly rises above  $10^8/\text{cm}^2$  (the onset of slip lines has little effect on the total dislocation density). Crystals examined on both sides showed that the dislocation density on the substrate side was substantially higher ( $\sim 10^8/\text{cm}^2$ ) than that on the growth side. This dislocation density is much higher than that in the MgO substrate ( $5 \times 10^5/\text{cm}^2$ ) and, together with the increase in density as the thickness decreases, suggests that dislocations are incorporated during the initial stages of growth rather than by propagation of defects from the substrate as suggested by Robinson *et al* [4].

### 3.2.2. Effects of Annealing on Crystal Perfection and Domain Structure

Annealing the NiO/MgO crystals at  $1450^\circ \text{C}$  simplifies the complex slip structures observed in as-grown crystals, and removes variations caused by different growth temperatures. Etching the cross-section of the NiO reveals a slip structure similar to that in MgO prior to annealing; the  $\langle 110 \rangle$  slip lines initiate at the interface and many extend to the growth surface. Examination of the surfaces of the NiO, after removal of the substrate, shows that the complex array of short slip lines on the back surface has been replaced by a relatively large-scale network of slip lines extending across the whole surface, and a similar network is seen on the growth surface of crystals less than  $\sim 130 \mu\text{m}$  thick.

Topographs taken from the back surface of the NiO reveal this slip network superimposed on the regular antiferromagnetic domain structure (fig. 8a), and this slip network is still visible above the Néel temperature, when the domain structure has disappeared. In general, topographs from the growth surface do not reveal the associated slip network with comparable contrast to that from the back surface, and it is often obscured by the domain structure (fig. 8b).

Previous work on the domain structure in these crystals [2] showed that, in addition to producing a very regular network of narrow domains, annealing on the substrate sometimes produced a large-scale network of wider or more complex domains (see fig. 3 of [2]). The present

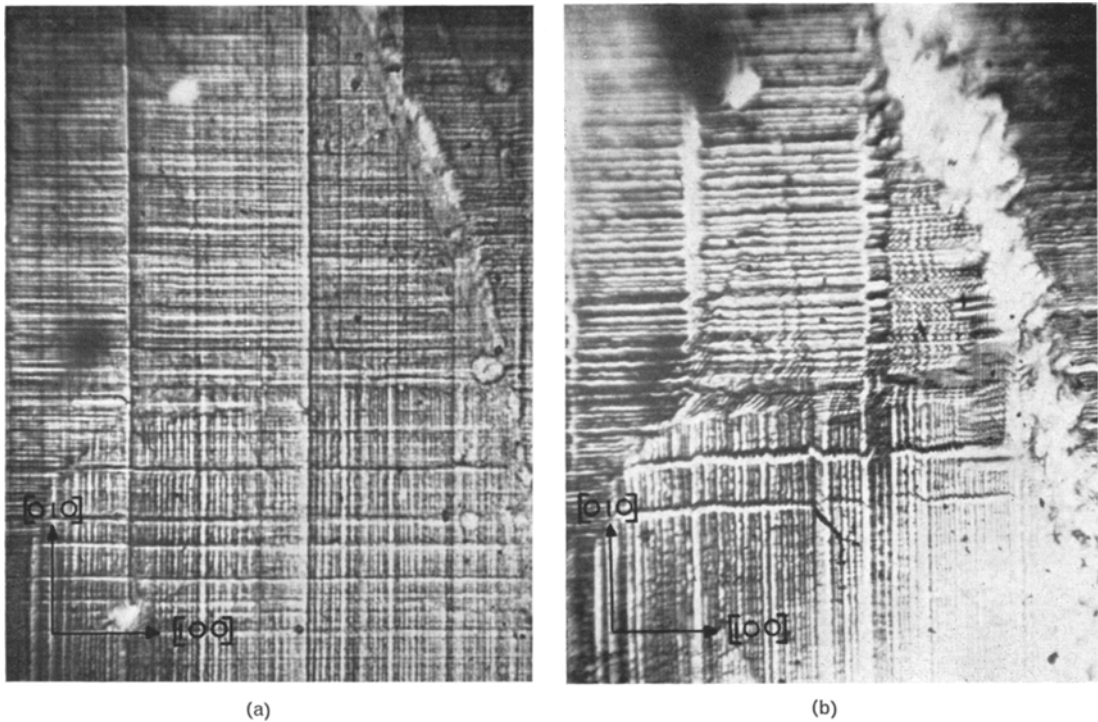


Figure 8 (a) Topograph of back face of NiO, previously annealed on the substrate, revealing the rectangular slip network superimposed on the domain pattern ( $\times 35$ ). (b) Topograph of growth surface of same region of crystal, showing the fundamental antiferromagnetic domain structure ( $\times 35$ ).

work has shown that this network is associated with the gross slip structure existing in these annealed crystals. In thin crystals ( $< 40 \mu\text{m}$ ) almost all of the slip bands affect the domain structure, but the effect becomes less marked as the crystal thickness increases. Moreover, the width of the wider domains are not equal to the crystal thickness, as they would be if the  $\{110\}$  slip planes influenced the domain structure over their complete length. In fact, the wider domains are separated from the slip traces in the growth surface in a direction towards the intersection of the slip plane with the interface. This suggests that it is only the high stress concentration associated with the slip planes in the vicinity of the interface that relaxes the restriction on very narrow domains [2], and the effect of this stress on the bulk domain structure decreases as the crystal thickness increases.

Annealing crystals previously removed from the substrate removes the plastic deformation observed in as-grown crystals. Etching shows no evidence of slip, although topographs occasionally reveal a faint large-scale structure on the back surface. The resulting domain behaviour is

similar to that in well-annealed melt-grown crystals where slight stress along  $\langle 111 \rangle$  can produce single domain crystals.

The overall dislocation density in crystals annealed on or off the substrate is lowered to about  $5 \times 10^6/\text{cm}^2$ .

### 3.2.3. Discussion

The dominant features associated with thick epitaxial films of NiO are (i) curvature of the crystal, (ii) dislocation networks, shown to be slip lines, and (iii) cleavage cracks. Cech and Alessandrini [6] observed cleavage and curvature, and tentative evidence of slip lines in the growth surface, all of which were attributed to the resulting strain after coherent growth and a direct result of lattice misfit. The lattice misfit between MgO and NiO at the growth temperatures used is about  $-0.75\%$ , which might have been responsible for the concave curvature observed in the NiO, were it not for the fact that work by the present authors on CoO deposited on MgO, also revealed a concave curvature of the CoO. Since the lattice misfit between CoO and MgO is  $+1.36\%$ , a convex curvature might

have been expected. Thus an alternative explanation is required for the induced strain and associated plastic deformation.

As the crystals cool from the growth temperature, stress will be induced at the interface due to differences in thermal expansion coefficients. The expansion coefficient of NiO (and CoO) is greater than that of MgO with the result that the NiO will cool under tension and the MgO under compression. This stress may cause the bicrystal to bend, producing the observed concave curvature and, as in the case of GaAs on Ge [5], cause the observed plastic deformation. Assuming that the interfacial strain is shared equally between the NiO and the MgO, the induced stress in either is approximately  $\sigma_f = Y\Delta\alpha\Delta T/2(1 - \mu)$  where  $Y$  is Young's modulus,  $\Delta\alpha$  the difference in thermal expansion coefficients,  $\Delta T$  the difference between the growth temperature and room temperature, and  $\mu$  is Poisson's ratio. Using published values for the above parameters, a growth temperature of 650° C, and making allowance for the anomalous changes in  $\alpha$  and  $Y$  near the Néel temperature [9], values of 12 and 3 kg/mm<sup>2</sup> are obtained for  $\sigma_f$  for MgO and NiO respectively. This value for MgO is greater than the quoted critical shear stress,  $\sigma_c$ , for glide in MgO [10] and hence sufficient to initiate slip and, although there are no quoted values for  $\sigma_c$  for NiO, the above value of  $\sigma_f$  is undoubtedly greater than  $\sigma_c$  since the shear modulus of NiO is some four times less than that for MgO. The rectangular nature of the  $\langle 100 \rangle$  slip traces observed in the back face of the NiO is a result of the symmetrical nature of  $\sigma_f$ , and the fact that the resolved shear stress is a maximum on  $\{110\}$  planes running at 45° from the interface to the growth face.

Cleavage normal to the interface in NiO and MgO increases with the thickness of the overgrowth due to the bending effect of the interfacial strain, and the bending is enhanced if cleavage occurs in the MgO parallel to the interface. Cleavage has never been observed at the interface itself, indicating the strength of the MgO/NiO bond.

#### 4. Conclusions

The present work has demonstrated that uniformly thick NiO single crystals can be grown epitaxially on to (001) cleavage faces of MgO over a wide range of substrate temperature, bromide vapour pressure and growth rate. The crystal thickness increases rapidly with increas-

ing growth temperature provided that the ratio  $P_W : P_B$  is within the range 50 to 16. The surface morphology of the crystals is more influenced by deficiency of water vapour or bromide vapour than by substrate temperature.

Modifications in growth technique introduced by Robinson *et al* [4], where the substrate and bromide are at different temperatures and multi-deposition is used to produce crystals thicker than 100  $\mu\text{m}$ , are felt to be unnecessary, since good quality, large area crystals of NiO have been grown by single deposition in a uniform reaction chamber temperature, from less than 2  $\mu\text{m}$  thick up to 400  $\mu\text{m}$ . However, for the growth of ferrites using similar techniques (cf Pulliam [11]), different temperatures for the various reagents and substrates may be necessary to ensure finite vapour pressures of all the constituents. The present results using an open system suggest that growth will occur over a wide range of substrate temperature, provided that the proportions of the individual vapours flowing over the substrate surface are within certain limits.

The macroscopic deformation observed in crystals grown above 650° C is believed to occur during cooling from the growth temperature, and it has been shown that the stress induced at the interface is sufficient for initiation. In addition to the anomalous changes in  $\alpha$  and  $Y$  in NiO in the vicinity of the Néel temperature, there is a structural change from cubic above to rhombohedral below the Néel point and the resulting symmetry difference between overgrowth and substrate must contribute to the interfacial stress. However, the formation of a large number of twin domains considerably reduces this additional strain [2] and any remaining effects have been neglected here. It is intended to extend this investigation to epitaxial CoO, grown by the same technique, to examine further the effects of the changes at the Néel temperature since this is below room temperature for CoO.

Annealing the NiO/MgO bicrystals removes localised stresses introduced during growth by imperfections, etc, and the stress due to differential thermal contraction induced on cooling produces regular macroscopic slip in both substrate and overgrowth. This gross deformation has been shown to directly influence the domain structure, whereas individual dislocations and small-angle boundaries have no effect on the regular domain structure observed in these crystals.



**References**

1. M. W. VERNON and M. C. LOVELL, *J. Phys. Chem. Solids* **27** (1966) 1125.
2. M. W. VERNON and F. J. SPOONER, *J. Materials Sci.* **2** (1967) 415.
3. M. FOËX, *Compt. rend.* **227** (1948) 193.
4. L. B. ROBINSON, W. B. WHITE, and R. ROY, *J. Materials Sci.* **1** (1966) 336.
5. H. HOLLOWAY and L. C. BOBB, *J. Appl. Phys.* **39** (1968) 2467.
6. R. E. CECH and E. I. ALLESSANDRINI, *Trans. ASM* **51** (1959) 56.
7. H. SHAFFER and H. JACOB, *Z. anorg. Chem.* **268** (1956) 56.
8. W. BERG, *Z. Krist.* **89** (1934) 286; C. S. BARRETT, *Trans. AIME* **161** (1945) 15.
9. K. P. BELOV, "Magnetic Transitions" (Consultants Bureau, New York, 1961) p. 132.
10. G. W. GROVES and A. KELLY, *Proc. Roy. Soc.* **275A** (1963) 233.
11. G. R. PULLIAM, *J. Appl. Phys.* **38** (1967) 1120.